Polymer 51 (2010) 3627–3635

Contents lists available at ScienceDirect

Polymer

journal homepage: www.elsevier.com/locate/polymer

Surface analytical approach to $TiCl_3$-based Ziegler–Natta catalysts combined with microstructure analysis of polymer

A.T.M. Kamrul Hasan [a,*], Y. Fang [b], Boping Liu [b], Minoru Terano [c]

[a] Chemical Engineering Laboratory, Department of Applied Chemistry and Chemical Engineering, University of Rajshahi, Rajshahi-6205, Bangladesh
[b] State Key Lab. of Chemical Engineering, East China University of Science and Technology, Mei Long Road, 130, Shanghai, P. C. 200237, PR China
[c] School of Materials Science, Japan Advanced Institute of Science and Technology, 1-1 Asahidai, Tatsunokuchi, Ishikawa 923-1292, Japan

ARTICLE INFO

Article history:
Received 7 March 2010
Received in revised form
19 May 2010
Accepted 26 May 2010
Available online 2 June 2010

Keywords:
Ziegler–Natta polypropylene catalyst
Isospecific active sites
Donor-free $TiCl_3$-based catalyst

ABSTRACT

In the field of Ziegler–Natta catalysis (ZNC), most of the previous works have been focused on the characterization of either catalyst surface or polymer microstructure but the combined studies of these two aspects are still limited. A clearer understanding concerning the isospecific nature of active sites on the donor-free $TiCl_3$ – based catalyst has been presented in this work in terms of both surface characteristics of the catalyst and microstructure of polypropylene (PP) produced. Ti- and Al-species existing in the catalyst surface have been identified by high resolution X-ray photoelectron spectroscopic (XPS) and solid-state magic angle spinning nuclear magnetic resonance (^{27}Al MAS NMR) techniques, respectively. Moreover, grinding effect on catalyst performance has been carried out to investigate the nature of active sites by particle size distribution (PSD) method. Microstructures of PPs produced using the surface characterized catalysts have been investigated by temperature rising elution fractionation (TREF), ^{13}C NMR and GPC methods. It can be demonstrated that the surface structure of catalyst is dominantly affected by the type of Al-alkyl cocatalyst used as well as the preparation method of catalyst whilst it precisely determine the nature of isospecificity of active sites and its distribution. Two different types of surface Ti^{+3}-species have been identified on the catalyst surface depending on the different vacant coordination states of surface titanium species. On the other hand, ^{27}Al MAS NMR experiments have shown the presence of surface aluminum in four (Al^{IV}), five (Al^{V}) and six (Al^{VI}) coordination number of multiple environments. The states of surface Al-species are sensitive to coordination number and symmetry of the local environment around the aluminum nuclei. Higher isospecificity of active sites is seen to be related to the higher fulfilled coordinated states of surface Ti- and Al-species.

1. Introduction

Since the discovery in the early 1950s, several generations of heterogeneous Ziegler–Natta catalysts (HZNC) with very high isospecificity and high activity have been successfully developed in the industrial circle by the introduction of different catalytic components such as, support materials, cocatalysts and electron donors making the whole catalyst system chemically complexed [1–4]. The world market for polypropylene (PP) production is currently over 20 × 10^6 tons and more than 80% of the global polymer is produced with HZNC. Despite the obvious industrial importance, many academic aspects regarding the mechanism of polymerization, the real origin of active sites, the exact structure of active sites and the role of various catalytic components on the stereospecific nature of active sites, the differences between the activities of the transition metal in various oxidation states of classical ZNC are largely yet to be clarified [5–15].

There have been numerous suggestions about the basic mechanisms of ZN olefin polymerizations. The commonly accepted mechanism of ZN catalysis is due to Cossee [16,17] wherein the active catalyst is assumed to have a vacant site to which monomer olefin binds to form metal-alkyl-olefin complex. The second, Green and Rooney's metathesis-type, holds that an alpha-hydrogen shifts from the growing polymer chain to the transition metal to form a metal carbine [18]. The third, Brookhart and Green's, holds that an alpha-hydrogen migrates only partially from the growing alkyl chain to the metal atom forming an agnostic bridge of CH–Ti [19]. The characterization of heterogeneous ZN catalysts has been attempted by means of several experimental approaches. Proceeded with the series of studies [20–34], the investigation on the

* Corresponding author. Tel.: +880 721 750041; mobile: 880 1714460001; fax: +880 721 750064.
E-mail address: alishaabir@yahoo.com (A.T.M.K. Hasan).

0032-3861/$ – see front matter © 2010 Elsevier Ltd. All rights reserved.
doi:10.1016/j.polymer.2010.05.053

isospecificity of active sites of the donor-free Ziegler–Natta catalyst provided the first evidence for the origin of active sites isospecificity from the catalyst substrate and the cocatalyst. These basic and profound understandings with respect to the stereospecific roles of cocatalyst and catalyst substrate gave rise to a good basis for further effort to elucidate the isospecific nature and structure of active sites on the catalyst surface as it replicates the polymerization mechanism and polymer microstructure. Most of these works deal with systems where titanium tetrachloride ($TiCl_4$) was supported on magnesium dichloride ($MgCl_2$) in the presence of an electron donor. But the effects of components of the catalyst system on the isospecific nature of active sites and the microstructure of polymer have not been well clarified. Busico et al. [35–41], in a series of papers, proposed the existence of two types of active sites depending on the support face acidity, Ti_2Cl_6 being the stereospecific one responsible for the isotactic chain propagation, while $TiCl_3$ the nonstereospecific one responsible for the random propagation. It is well recognized that HZNC are composed of multiple active sites, which produce polymer with varying degree of stereoregularity. Although there are many different types of HZNC, most have a common intriguing characteristic: they yield polymer with broad molecular weight distribution (MWD) and in the case of copolymerization, broad chemical composition distribution (CCD). According to Keii [42,43], the abnormally broad MWD is primarily caused by a non-uniform physical or chemical structure of the catalyst. The non-uniform nature of the heterogeneous ZN catalysts was reported by several authors with the aid of advanced surface analysis methods [44–53]. Despite considerable efforts with different surface analysis methods, it has not been possible to determine the exact structures of the both isospecific and non-isospecific active sites [54].

In addition to the experimental work, a lot of theoretical studies have also been devoted to the investigation of the ZN polymerization. Theoretical methods provide an attractive alternative. A number of calculations studying some form of HZNC with titanium as the main component of the active site have been published [4,55–70]. Recently, some progress has been achieved with molecular modeling methods [10,61,71], but more common is an indirect approach to study the polymer structure. Several models have been proposed to describe the structure of the isospecific and of the aspecific active sites. Among them, Corradini's model [72–76] is in good agreement but it seems too simplified [7] when it describes the function of donor effects. In fact, as already observed by other authors, this model does not explain some experimental data such as the variations of molecular weight and molecular weight distribution [77], tacticity distribution [78,79] etc. As recently reviewed by Soares [80], the general mathematical methods for modeling olefin polymerization have been well established. For a HZNC, a model with finite number of site types is assumed. Each of these sites has distinct kinetic constant for the initiation, propagation, chain transfer, deactivation and catalyst poisoning reactions. While these calculations have provided significant insight into the nature of the catalysts, they have not as yet resolved the particular agreement on the exact structure of the active sites on the catalyst surface and/or their physico-chemical stability.

Extensive studies of literature review on HZNC have been made to travel the basic steps in the catalytic process, a deeper understanding of the structure of the active centers, the role of the supporting surfaces is still needed and the oxidation states if Ti-species when adsorbed on the surface structures are still under discussion [81,82]. A comprehensive survey of polymerization at the various active sites has yet to be done, however. Indeed, these factors play a crucial role in determining the activity and nature of the isospecificity of active sites in the olefin polymerization reaction. To begin with this challenge, a previous study [83,84] has been performed for a basic understanding concerning the isospecific nature of active sites on $TiCl_3$-based catalysts from the yield and other characteristics (tacticities by ^{13}C NMR, tacticities distribution by TREF, molecular weight and molecular weight distribution by GPC) of PP produced at various catalyst preparation method, catalyst-cocatalyst ratios, temperature and preactivation procedure of catalyst-cocatalyst mixture. Since, most of the above mentioned studies concerning the types of active sites model have been based on information from either characterization of microstructures of PP or from surface analytical approach to catalyst surface [11,12,85]. Clear evidence on the exact structure of isospecific active sites is expected to be relating not only to the microstructure analysis of the PP but also to the catalyst surface structure. Therefore, the present work focuses on the surface characterization of two-components donor-free $TiCl_3$/Al-alkyl catalyst (to avoid the complexity of the catalyst system) and its correlation to the microstructure of polymer produced with the same catalyst systems. The key concept of this study is to elucidate the (i) variation of coordination states in the surface titanium species (ii) chemical structure of the titanium active center (iii) which titanium species is isospecific (iv) which titanium species is non-isospecific (iv) various coordinative states of surface aluminum species on the solid catalyst. From the academic and scientific point of view, these are the main novelty of the present work.

From the practical point of view, it is considered that high resolution XPS has great potentials as an effective tool for understanding the oxidation states and the distribution of the titanium species before and after the reaction with the Al-alkyl cocatalyst. High-resolution ^{27}Al MAS solid state NMR spectroscopy, with recording spectra in high magnetic fields and use of special methods to narrow the NMR lines of the solid samples, might be the second most promising method to study the coordinative states of Al-species on catalyst surface. Moreover, particle size distribution (PSD) analysis of catalyst has been carried out to investigate the grinding effect on the surface structure of active sites as well as production yield of PP. For a meaningful correlation with the surface structure of active species, it is important that the structure of polymer produced by individual active site types should be described as accurately as possible through tacticity, tacticity distribution, molecular weight and molecular weight distribution measured by ^{13}C NMR, TREF and GPC techniques, respectively as it replicates the catalyst surface structure of active sites.

2. Experimental

2.1. Raw materials

Research grade propylene (Chisso Corp.) was used without further purification. Anhydrous AA-$TiCl_3$ was supplied by Toho Titanium Co. Ltd. Molecular sieves 13X (Wako Pure Chemical Industries, Ltd.) were used as moisture scavengers for solvent purification. Heptane and toluene (Wako Pure Chemical Industries Ltd.) solvents were purified by passing through molecular sieves 13X column. Triethylaluminum (TEA) and diethylaluminum-chloride (DEAC) (Tosoh Akzo Corp.) and nitrogen (Uno Sanso Corp.) were used without purification. TEA and DEAC were used after dissolving in toluene solvent.

2.2. Catalyst preparation

Wet ground (WG) processing of AA-$TiCl_3$ catalyst was performed by milling 36 g of supplied catalyst in a ball mill with 200 ml heptane and dry ground (DG) processing was performed in the same way without heptane. The grinding of catalyst was carried out

in a 1.2 L stainless steel pot containing 55 balls each of 25 mm diameter for 30 h at room temperature. The processed catalysts were obtained as heptane slurry. The entire process was performed under nitrogen atmosphere. Titanium content in the catalyst slurry was determined by the redox titration method. The catalyst slurry was then kept in a three-necked round-bottomed flask equipped with a magnetic chip under nitrogen atmosphere.

2.3. Particle size distribution (PSD)

PSD characterization of both WG and DG $TiCl_3$ catalyst was carried out by ablating matter with Q-switched Nd:YAG laser and transporting ablating material to a particle counter for sizing by light scattering. PSD measurement is based on the measurement of the frequency distribution of diameter of particle sections. The number of size intervals into which the particles should be classified depending on the width of the distribution and is to some extent a matter of choice. The number of particle, which should be counted for obtaining a satisfactory picture of the distribution also depends on the range of sizes present in the specimens under study. The histogram of the PSD was obtained as a curve of particle size (μm) vs. relative intensity (%) and integral line (wt%).

2.4. Surface characterization by XPS

The ultra high vacuum (UHV) chamber used in this study was equipped with a sputter ion gun for surface cleaning, an X-ray source and a double pass cylindrical mirror analyzer (CMA) with a coaxial electron gun for X-ray photoelectron spectroscopy (XPS). The XPS data of the catalyst was taken by Physical Electronics Perkin–Elmer (Model Phi-5600 ESCA) spectrometer with monochromated Al Kα radiation (1486.6 eV) operated at 300 W. It was carried out in a glove bag under nitrogen atmosphere. The sample holder was then put into a vacuum transfer vessel (Phi Model 04-110, Perkin–Elmer Co., Ltd.), which is connected to the sample introduction chamber of the XPS instrument. The sample was degassed up to 10^{-7} Torr. The main chamber vacuum was kept above 5×10^{-9} Torr during XPS data acquisitions. A neutralizer was used to reduce the charging effect in order to obtain a better signal to noise ratio. All binding energies (BE) were referenced to the Au $4f_{7/2}$ peak at 84 eV to correct for the charging effect during data acquisition. Multiplet fittings of the Ti 2p XPS curves were carried out by the Gaussian–Lorentzian method to determine the mixed states of valences in all the samples. The binding energy (BE) and the full width at half maximum (FWHM) values from the Ti 2p XPS spectra was measured and used as criteria for identification of the oxidation state, distribution state and existing state of surface Ti-species on catalyst surface. The XPS spectra of Ti 2p have been deconvoluted into a series of synthetic peaks (67% Gaussian and 33% Lorentzian; FWHM = 2.3 eV) that represent the photoelectron emission from different oxidation states. The fitting for each curve was repeated to ensure a reproducible result.

2.5. Characterization by solid state NMR

The AA-$TiCl_3$ catalyst was treated by a cocatalyst within a glove bag under nitrogen atmosphere. Dried AA-$TiCl_3$ catalyst and cocatalyst-activated AA-$TiCl_3$ catalysts (ca. 200 mg) were successively introduced into a 7 mm silicon nitride MAS rotor. The ^{27}Al MAS solid state NMR spectra were measured by a Varian UNITY-400 spectrometer operating at 104.35 MHz at room temperature with a Varian RT/CP MAS probe. The ^{27}Al MAS solid state NMR was recorded for sample rotating at ca. 5 kHz using 7-mm silicon nitride rotors. The spectra were obtained with a 12° pulse of 1.75 μs and a relaxation delay of 0.2 s. The chemical shift was referenced to an external standard of a 1 M aqueous solution of $Al(NO_3)_3$ for the ^{27}Al NMR spectroscopy. The strongest ^{27}Al MAS solid state NMR signal of the silicon nitride rotor at 100 ppm was used as the internal standard peak for chemical shift corrections of all spectra obtained from various activated catalysts.

2.6. Propylene polymerization

Polymerization experiments were carried out in a three-necked 300 ml round-bottomed flask reactor equipped with a magnetic chip. After nitrogen purging and heating, successive introduction of heptane solvent, Al-alkyl cocatalyst, catalyst slurry and propylene monomer were done. The conditions for polymerization were maintained as: 2 mmol Ti (slurry 5.65 ml), Al/Ti molar ratio 3, heptane volume 138.35 ml, cocatalyst 6 ml, total volume 150 ml, temperature 40 °C and time 30 min. Polymerization was allowed to stop by introducing ethanol–water after experimental time. The polymer slurry was kept into ethanol–water for 12 h with stirring. Then it was successively washed with deionized water, dried at room temperature, dissolved in orthodichlorobenzene (ODCB) with heating, and reprecipitated into ethanol–water and then followed by filtration and drying in the vacuum dryer at 60 °C until a constant weight was obtained.

2.7. Tacticity measurement by ^{13}C NMR

To measure the ^{13}C NMR spectroscopy, the sample was prepared by dissolving polymer in a mixture of hexachloro-1,3-butadiene as a diluent and 1,1,2,2-tetrachloroethane ($C_2D_2Cl_4$) as a reference. The spectra of the samples were recorded at 120 °C on a JEOL GSX-270 spectrometer operating at 67.8 MHz, relaxation delay 8s, number of pulses 6000, pulse angle 90°, spectrum width 16,000 Hz, and spinning speed 15 Hz. The chemical shift was represented in ppm downfield from internal $C_2D_2Cl_4$ (74.3p). The tacticity of PP was determined from the area of the resonance peaks (19.5–22.0 ppm) of the methyl region and pentad sequences were represented by mmmm = meso pentad and rrrr = racemic pentad respectively.

2.8. Tacticity distribution by TREF

TREF analysis was performed with an on-line system (Senshu SSC-7300) with orthodichlorobenzene (ODCB) containing 0.03 wt% of 2,6-di-tert-butyl-4-methylphenol (butylhydroxytoluene, BHT) as an antioxidant. A fractionation column packed with Chromosorb (Celite Corp.), 10 mm in diameter and 30 cm in length, was used for this analysis. PP sample was dissolved in 10 ml ODCB at 140 °C with continuous shaking and a part of the PP solution (ca. 6 ml) was passed through the fractionation column, which was then slowly cooled down at 6.7 °C/h from 140 to 20 °C. The deposited polymer was eluted with ODCB in a flow rate of 2.5 ml/min at 20 °C for 30 min to obtain the ODCB-soluble fraction and then the column was heated at 16 °C/h from 20 to 140 °C to elute the consecutive higher isotactic polypropylene. The output result, detected with an infrared (IR) detector operating at a wavelength of 3.41 μm, was presented as a fractogram normalized to a constant area.

2.9. MW and MWD by GPC

The molecular weight (MW) and molecular weight distribution (MWD) of polypropylene samples produced were determined by gel permeation chromatography (GPC) method (GPC, Senshu SSc-7100) with polystyrenes gel columns (Tosoh TSK-GEL G3000HHR and TSK-GEL G5000HHR) at 140 °C using o-dichlorobenzene (ODCB) as a solvent. MW was calculated with a universal calibration curve based on polystyrene standards with narrow MWDs

using appropriate Mark–Houwink constants. The resolution of GPC curves as deconvolution into Flory components was performed with the MicroMath Scientific computer programs software. Instantaneous MWD of polypropylene made with multiples type catalyst as a superposition of four individual Flory most probable MWDs were indicated by solid line of the whole polymer and by dotted lines of the polymers made on distinct active site types.

3. Results and discussion

A typical XPS result, shown in Fig. 1, has described the XPS spectra of the Ti_{2p} region of (a) original AA-$TiCl_3$, (b) DG AA-$TiCl_3$ and (c) WG AA-$TiCl_3$ catalysts to rationalize the grinding effect on the nature of the active sites. The constituent atoms of the catalyst (Cl, Ti, C, Al) were observed on the XPS measurable surface, approximately 2 nm in sampling depth. To investigate the states of the titanium species in detail, high resolution XPS narrow scans of the Ti_{2p} region were performed for each catalyst. The doublet at two different binding energies (split between two peaks with an intensity ratio of 2:1) is reported to be due to spin-orbit coupling effects in the final state of the emitted electron. The doublet at 458.5 and 464.6 eV are reported to be due to the Ti $2p_{3/2}$ and Ti $2p_{1/2}$ photoelectrons from titanium atoms in it molecular states [86,87]. Thus, the doublet shown in the XPS spectra is ascribed to the $2p_{3/2}$ and $2p_{1/2}$ photoelectrons [88] from titanium atoms existing in the AA-$TiCl_3$ catalyst.

It is seen that all catalyst systems indicate two computer-simulated peaks in the region of Ti $2p_{3/2}$ spectra, which can be ascribed by the two kinds of Ti-species on the catalyst surface depending on the different levels of the coordination states of the surface titanium species. One of the Ti-species at a higher binding energy is assigned to the lower coordinated titanium species Ti^{3+}(a) with higher coordination vacancies whereas another at a lower binding energy is considered to be the higher coordinated titanium species Ti^{3+}(b) with lower coordination vacancies [51]. The plausible structures of these two kinds of surface titanium species are displayed in Scheme 1. Usually, the divalent titanium species exists on the catalyst surface by sharing two chlorine atoms (through chlorine-bridge) with other titanium or aluminum. Thus, the catalyst crystal may be considered as built up of elementary sheets, each consisting of two chlorine layers sandwiching a titanium layer.

According to the literature [89], at the surface of $TiCl_3$ catalyst, two kinds of surface sites are possible:

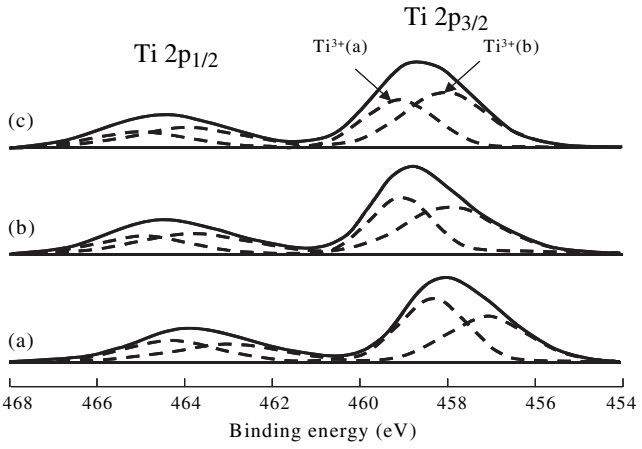

Fig. 1. The Ti 2p region of the XPS spectra. (a) Original AA-$TiCl_3$, (b) DG AA-$TiCl_3$, (c) WG AA-$TiCl_3$.

(i) The first type has one chlorine vacancy and two loosely bound chlorine atoms.
(ii) In the second type, there are two chlorine vacancies and one loosely bound chlorine atom.

Due to surface heterogeneity of the catalyst [90], titanium species may also remain on different surface locations and may exhibit different tendencies in the formation of active sites. Thus, low coordinated Ti^{3+} with two or three vacant sites can be possibly present in solid state, mainly situated at the edges and corners of the crystallite's surface. According to the literature [91], the active centers of titanium species are contained on the lateral planes, as the not completely coordinated titanium atoms which are the most liable to the formation in the proximity of a crystal defect [92] of the metal–carbon bond are situated on those planes where the titanium atoms are accessible without steric hindrance. On the other hand, the main plane, which forms 95% of the catalyst surface may be considered passive from the point of view of the polymerization process. Okura et al. [93] examined a polymerizing system microscopically, and found that both fibrous and lamellar polymer growths could be observed. It has often been supposed that two types of polymerization centers exist in $TiCl_3$, and in addition to these direct observations, John Boor [94] assumed the existence of two different structures for active centers to account for the formation of both isotactic and atactic polymers during Ziegler–Natta polymerization. According to Arlman et al. [95], the active sites are localized on the surface of the $TiCl_3$ catalyst due to the surface chlorine vacancy sites, which should be formed to keep the crystal in an overall electroneutral state. The XPS signals show that the peak has shifted to the higher binding energy due to the decrease of the coordination state of all surface titanium species after grinding. Shifts in BE have a contribution from both the oxidation state and the charge on the nearest neighbor atoms of the excited atom. The chemical shift and the FWHM of the $2p_{3/2}$ peak in XPS analysis of Ziegler–Natta catalysts indicate the electron density of the titanium species, namely the oxidation state and its distribution, respectively [51]. Therefore, the results of the XPS data analysis in terms of binding energy (BE), full width and half maximum (FWHM), oxidation states, and atomic percentage of surface titanium species are listed in Table 1.

From the XPS data analysis of these catalyst systems, it can be seen that after interaction with the cocatalyst the binding energy of the Ti^{3+}(b) species has decreased, which may be due to the association of the electron donating alkyl groups with the surface Ti-species [51]. It can also be speculated that the weakly bonded surface chlorine atoms can be replaced by the electron donating ethyl group of the cocatalyst. The increase in binding energy is due to the formation of a coordination vacancy by the extraction of dangling Cl on the catalyst surface induced by the grinding effect. Thus, the DG catalyst has a binding energy higher than that of the WG catalyst even though the atomic percentage of higher coordinated Ti^{3+}(b) has not changed significantly between these two catalyst systems. In the WG catalyst, active species mostly remain on the crystalline layers, which correspond to the titanium species with a higher coordination state (lower Cl vacancy), whereas in the DG catalyst, the active species are mostly located at the edges and defects of the catalyst, which corresponds to the lower coordination state (higher Cl vacancy). The most striking effects of dry grinding is the drastic crystallographic changes induced by shear forces that are strong enough to cause sliding at the metal-free interfaces of the Cl–Ti–Cl double layer; this leads to disorder in the stacking, which essentially becomes random after prolonged intense dry grinding [96–98]. According to the literature [99], the electron deficient catalytic species are suggested to be responsible for the binding energy increase. It can be

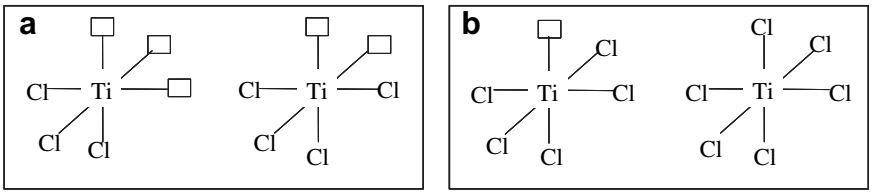

Scheme 1. Isospecific nature of active sites relating to the coordination states of surface titanium species. □: Coordination vacancy.

seen that after grinding, the atomic percentage of surface titanium species Ti^{3+}(b) with higher coordination states has significantly increased (about 10%). This is because of the grinding effect of catalyst, catalyst particles are disintegrated into small particles exposing more surface layers as well as Ti-species with higher coordination states.

Although the surface area could be increased due to the break of the large particles into smaller ones, the newly-exposed surface Ti-species are mainly situated on the newly-exposed crystalline surface rather than on the newly-exposed edges or corners of the small crystallites. Therefore, the grinding increased the ratio of high coordinate Ti^{3+}. According to the literature [100a] grinding markedly disrupts the crystal bonding structure at least on the surface of the crystals, as indicated by the appearance of an ESR signal of Ti (III) after grinding. The surface of ground $TiCl_3$ may therefore be rather rough, so that the number of active sites (e.g. exposed Ti) can be considered to be the same order of magnitude as the number of surface Ti atoms.

However, the WG catalyst shows a slightly higher atomic percentage of Ti^{3+}(b) species, caused by making more layer-wise fragmentation and a less defective catalytic surface than that of the DG catalyst. According to Mejzlik and co-authors [101], the grinding of $TiCl_3$ in hydrocarbon medium not only increases the specific surface but also causes a basic change in the reactivity of the $TiCl_3$ surface. To investigate the effect of Al-alkyl cocatalyst on the coordination states of surface titanium species, XPS analysis was also performed for the WG AA-$TiCl_3$ catalyst before and after reaction with TEA or DEAC. The XPS spectra of these catalyst systems are shown in Fig. 2. After interaction with the cocatalyst, the peak intensity of the higher coordinated Ti^{3+}(b) species has drastically decreased in comparison to that of the titanium species obtained from the WG AA-$TiCl_3$ catalyst. TEA shows a more drastic decrease of the peak intensity of the Ti^{3+}(b) species and at the same time increased the peak of Ti^{3+}(a) species (Fig. 2b) but DEAC did not show a big change (Fig. 2c). XPS data analysis also shows that the atomic percentage of Ti^{3+}(b) species has decreased to about 70% after interaction with TEA and to about 32% with DAEC. This explanation is that TEA as a cocatalyst has remarkably transformed the higher coordinated titanium species Ti^{3+}(b) into a lower coordination state titanium species Ti^{3+}(a) due to its stronger reactivity than that of DEAC.

Moreover, another explanation can be explored for the drastic decrease of surface atomic percentage of Ti^{3+}(b) species, which may be due to the extraction of surface dangling Cl by the effect of a cocatalyst. The extraction of surface dangling Cl is significantly affected by the effect of TEA, which shows a lower percentage of Ti^{3+}(b) species (only 18.84%), while DEAC shows higher percentage of Ti^{3+}(b) species (41.87%). By the way, another point possibly associated with the slight decreasing of the average binding energies of those Ti-species after Al-alkyl cocatalyst treatment might be the possible reduction of a small fraction of Ti^{3+}(b) into Ti^{2+}, which had not been considered in the previous explanations. The over-reduction of Ti (from Ti^{3+} to Ti^{2+}) [102] becomes inactive especially for propylene polymerization. Here, it is worth-while using XPS observation to detect the difference in the titanium species in terms of coordination number produced by the reaction with various alkylaluminums [51] suggesting that the variation in the coordination state of the titanium species is closely related to the reactivity of the alkylaluminum. The binding energy (BE) decreased, indicating the progress of the reduction of the titanium species on the catalyst. It is well known that surface Ti-species of heterogeneous Ziegler–Natta catalysts are first reduced and then alkylated by the effect of the cocatalyst. The FWHM of the Ti $2p_{3/2}$ peaks of both Ti-species show different values after grinding and reacting with the cocatalyst, suggesting the different chemical environment of the catalyst surface. In fact, however, the alkylaluminum cocatalyst interacts with the heterogeneous Ziegler–Natta catalyst through the ligand change of the surface Ti-species [33].

In the case of heterogeneous Ziegler–Natta catalysts, the ^{27}Al MAS NMR method could be expected to give one more bit of significant information regarding the nature of the isospecificity of active sites through the investigation of the coordinative states of

Table 1
The XPS data analyses from multiplet fitting of Ti 2p spectra of AA-$TiCl_3$ catalysts.

Catalyst system	Ti $2p_{3/2}$		Oxidation state	Atomic percentage
	BE (eV)	FWHM (eV)		
Original AA-$TiCl_3$	458.33	1.81	Ti^{3+}(a)	51.39
	457.07	2.20	Ti^{3+}(b)	48.61
WG AA-$TiCl_3$	459.02	1.69	Ti^{3+}(a)	40.09
	457.88	2.62	Ti^{3+}(b)	59.92
DG AA-$TiCl_3$	459.09	1.95	Ti^{3+}(a)	40.41
	458.02	2.29	Ti^{3+}(b)	59.58
WG AA-$TiCl_3$/TEA	458.83	1.54	Ti^{3+}(a)	81.16
	457.48	1.70	Ti^{3+}(b)	18.84
WG AA-$TiCl_3$/DEAC	458.77	1.67	Ti^{3+}(a)	58.14
	457.52	1.82	Ti^{3+}(b)	41.87

Ti^{3+} (a) stands for Ti^{3+} species with lower coordination states.
Ti^{3+} (b) stands for Ti^{3+} species with higher coordination states.

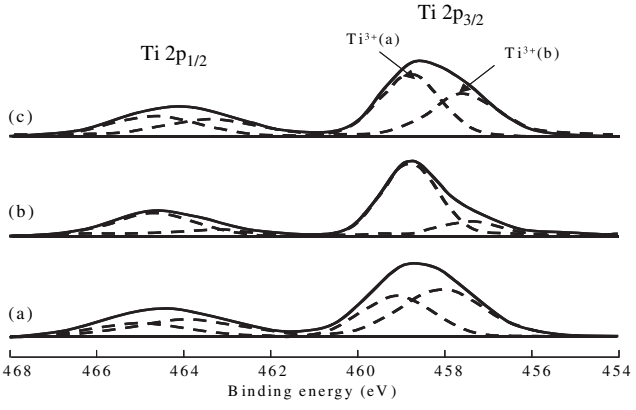

Fig. 2. The Ti 2p region of the XPS spectra. (a) WG AA-$TiCl_3$, (b) WG AA-$TiCl_3$/TEA, (c) WG AA-$TiCl_3$/DEAC.

an alkylaluminum cocatalyst [100a,103]. In this work, the ^{27}Al MAS NMR technique has been used to investigate the role and coordinative states of an alkyl-Al cocatalyst on the AA-$TiCl_3$ catalyst in order to further elucidate the mechanistic aspects of the cocatalysts in creating a multiplicity of active sites. This technique allows the identification of aluminum environments in four, five and six coordinations for different aluminum sites as a far more effective characterization of the Al^{IV}, Al^{V}, and Al^{VI} environments on the catalyst. Fig. 3 shows the ^{27}Al MAS NMR spectra of (a) pure $AlCl_3$ (b) WG AA-$TiCl_3$ (c) WG AA-$TiCl_3$/DEAC and (d) WG AA-$TiCl_3$/TEA catalyst systems. It has been demonstrated that the chemical shifts of ^{27}Al MAS NMR spectra vary with not only the coordination number of the aluminum species but also the types of adjacent ligands [104]. The solid state NMR investigation provides the local environment of the aluminum species on the catalyst surface. The signals position and intensity situated at the chemical shift approximately 0 ppm in the ^{27}Al MAS NMR spectra of pure $AlCl_3$ (Fig. 3a), WG AA-$TiCl_3$ (Fig. 3b), DEAC reacted WG AA-$TiCl_3$ (Fig. 3c), and TEA reacted WG AA-$TiCl_3$ (Fig. 3d) catalysts are assigned to the six-coordinated aluminum-containing compound.

It can be seen that when DEAC is used as a cocatalyst, the signal at 0 ppm of six-coordinated aluminum compound is dominant. This signal nicely corresponds with the ^{27}Al NMR data for $AlCl_3$ in crystalline form (0 ppm). For the DEAC activated catalyst, it can be seen that the dominant Al-species on the DEAC activated catalyst is six-coordinated and the direct coordination of the DEAC with the catalyst surface is relatively strong. A chemical shift of 0–10 ppm corresponds to the octahedral coordination of aluminum, that of 25–35 ppm to pentahedral coordination, and 60–100 ppm to tetrahedral coordination [103]. When TEA is used as a cocatalyst, the signal in ^{27}Al MAS NMR spectra of the WG AA-$TiCl_3$ catalyst corresponding to six-coordinated aluminum species drastically decreased and new signals with strong intensity appeared at approximately 55 and 75 ppm in the ^{27}Al MAS NMR spectra. These new signals at higher chemical shift (lower field) of aluminum peaks are ascribed to the lower coordination numbers of aluminum compounds in the catalyst system. For TEA reacted catalyst surface, the peaks around 0 ppm also show lower intensities compared with the standard peak. These results indicate that the Al-species on the TEA activated catalyst is dominantly assigned to four- and five-coordinated compounds. The results also suggest that some of the aluminum compounds are transformed into one another on the catalyst surface or that the coordination environment of aluminum in this compound became disordered. It could be concluded that Al-species from the interaction with DEAC are mainly six-coordinated and Al-species from the interaction with TEA are mainly 4- and 5-coordinated.

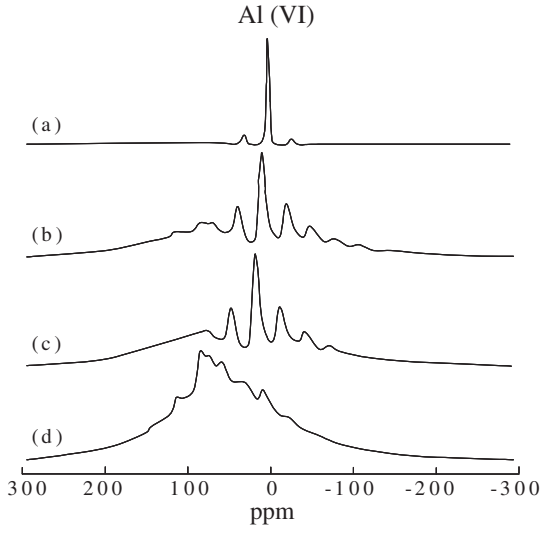

Fig. 3. ^{27}Al magic angle spin (MAS) solid state NMR spectra. (a) $AlCl_3$, (b) WG AA-$TiCl_3$, (c) WG AA-$TiCl_3$/DEAC, (d) WG AA-$TiCl_3$/TEA.

To support the above experimental results, some reports [105,106] regarding the assignment of various aluminum compounds could be introduced as references. A comparison of the chemical shifts of $AlCl_3$, $AlEtCl_2$, and $AlEt_2Cl$ solutions shows that as an organic ligand replaces an inorganic one in compounds with the same aluminum coordination, the line shifts to a lower field (chemical shift increases). The line at 70–80 ppm is attributed to the four-coordinated aluminum surrounded by chlorine atoms or five-coordinated aluminum with two ethyl groups. The line at 35 ppm can arise from the six-coordinated aluminum with three ethyl groups in the $(DEAC)_n$ chains forming on the support surface. The line at 0 ppm most likely corresponds to the six-coordinated aluminum with four chlorine atoms and two ethyl groups. The observed differences in chemical shifts of all four- five- and six-coordinated aluminum atoms between the catalyst systems are probably due to the difference in coordinative ligands. It can therefore be concluded that there are three types of aluminum species on these catalysts, namely 4-, 5- and 6-coordinated aluminum species, which originated from the interaction with different cocatalysts on the surface Ti-species.

Up to now, the surface characterization results of AA-$TiCl_3$ catalyst have been discussed in terms of the coordination states of surface Ti-species and surface Al-species concerning the catalyst preparation methods and types of cocatalysts. Later sections will focus on the polymerization results and microstructure analyses of polymers produced with these catalysts in order to make a correlation between the surface characterization of the catalyst and the microstructure of the PP. Some results of slurry polymerization data, activity, tacticity of polymer measured by ^{13}C NMR, are also listed in Table 2.

Since the polymer replicates the catalyst particles, there is sharp relationship between the morphology of polymer and the morphology of the catalyst used to produce them [107]. It is observed that polymerization with unground original catalyst provided low activity due to very low catalyst surface area but polypropylene produced showed very high isotacticity due to undisturbed regular arrangement of active species on catalyst surface structure. According to Cossee [108], high stereospecificity of $TiCl_3$ catalyst means that the stereospecific position of Cl atoms on $TiCl_3$ catalyst controls the coordination direction of monomer insertion during polymerization. TEA as a cocatalyst shows higher activity due to a strong alkylating ability whereas DEAC shows lower activity due to weak alkylating power. The catalyst systems using TEA usually show much higher polymerization activity but much lower tacticity in comparison with those using DEAC. From the Table 2, it is seen that WG catalyst produced higher

Table 2
The dependence of activity and pentad fractions of PPs produced with AA-$TiCl_3$ catalyst systems. (Polymerization condition: Ti content: 2 mmol, Al/Ti: 3, temperature: 40 °C, time: 30 min, solvent: heptane).

Catalyst system	Activity (g-PP/g-Ti·h)	Isotacticity[a] (%)			
		mmmm	mmmr	mmrm	mrrm
Original AA-$TiCl_3$/TEA	4.98	97.2	1.8	1.0	0.0
Original AA-$TiCl_3$/DEAC	1.32	98.6	1.4	0.0	0.0
WG AA-$TiCl_3$/TEA	86.4	72.1	8.3	10.2	9.3
WG AA-$TiCl_3$/DEAC	14.4	93.6	4.7	1.7	0.0
DG AA-$TiCl_3$/TEA	29.8	65.2	11.0	12.6	11.2
DG AA-$TiCl_3$/DEAC	10.2	87.5	7.2	3.1	2.2

[a] Measured by ^{13}C NMR, m = meso, r = racemic.

polymerization activity and isotacticity than DG catalyst. This is mainly due to the grinding effect that can be explained from the PSD results in the next section. The PSD curves of two catalysts are shown in Fig. 4.

The catalyst preparation method in terms of either WG or DG was found to be the second most important factor in determining the isospecific nature of active sites and polymerization activity. However, WG catalyst shows narrow particle size distribution curve (Fig. 4a) with average particle size of 3 μm than a DG catalyst having broad particle size distribution curve (Fig. 4b) with average particle size of 18.22 μm. WG catalyst with higher surface area due to finer particle sizes provided higher polymerization activity than DG catalyst. According to the report of Chien et al. [109], an increased surface area (149 m^2/g) with each step of the catalyst preparation was found from the measurement of nitrogen sorption of catalyst at room temperature. Active sites in heterogeneous Ziegler–Natta catalysts are usually situated on the catalyst surface. As a result, the increase of the catalyst surface area by grinding, if performed properly and under pure condition, always results in a more or less proportional increase of catalyst activity [21,110–112]. Another article [113] provided information that the specific surface area of $TiCl_3$ catalyst ground for different periods of time was determined by BET method. The maximum surfaces obtained under different conditions of grinding was obtained 25–27 m^2/g in comparison to the specific surface area 6 m^2/g of original catalyst.

The tacticity distribution of PPs produced by different catalyst systems have been measured by TREF method and presented in Fig. 5. From TREF analysis, it is observed that completely atactic fraction eluted at 20 °C whereas perfectly isotactic fractions eluted in between 115 and 120 °C temperatures and in between 20 and 115 °C, less isotactic fractions are eluted. According to the literature [114], the melting temperatures and isotactic pentad fractions for the individual fractions, both increased linearly with an increase in elution temperature, fractionation takes place according to isotacticity. However, from the TREF analyses it can be said that $TiCl_3$/TEA catalyst system produces dominantly aspecific active sites accompanied with a certain amount of the highest isospecific active sites and a few amount of less isospecific active sites. On the other hand, $TiCl_3$/DEAC catalyst systems primarily contain the highest isospecific sites, together with a few aspecific active sites and less isospecific active sites. Therefore, it can be concluded that the nature of the isospecificity of active sites is dominantly affected by the roles of cocatalyst types and catalyst preparation methods.

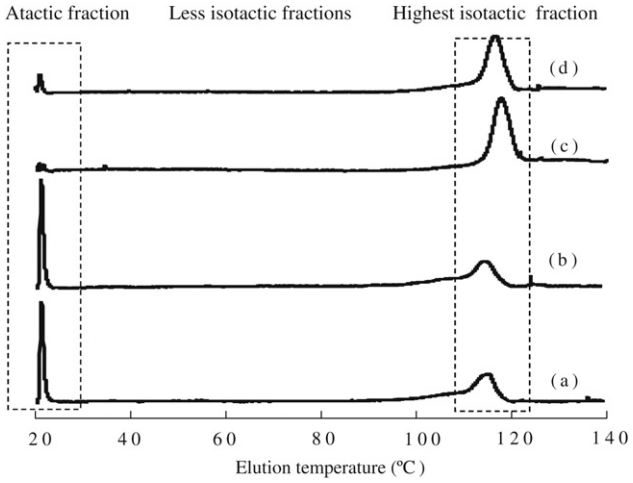

Fig. 5. Temperature rising elution fractionation diagrams of PPs produced from donor-free AA-$TiCl_3$ type catalyst with Al/Ti molar ratio = 3 at 40 °C for 30 min polymerization. (a) WG-TEA, (b) DG-TEA, (c) WG-DEAC, (d) DG-DEAC.

PPs produced with WG $TiCl_3$/TEA and WG $TiCl_3$/DEAC catalyst systems were characterized by GPC method. The deconvoluted average MW and MWD curves are shown in Fig. 6. Four types of Flory components (F1, F2, F3, and F4) were identified to describe the different types of non-uniform active sites correlating to the different molecular weight distribution of deconvoluted GPC curves of polymer.

It is notable that the microstructure analysis of the polypropylene samples were carried out by measuring the molecular weight and molecular weight distribution using GPC method and the curves were fitted by multiple Flory most probable distributions. The number of Flory peaks was correlated to the number of active sites and changes in the relative intensities of the different peaks were used as an indicator of the changes in active site distribution. It is well known that multiple active sites exist in heterogeneous Ziegler–Natta catalysts [115], including the $TiCl_4$/$MgCl_2$ based high-yield supported catalysts. In most cases, 3–6 types of active sites can be identified [116,117], and each of them is able to produce polymer with molecular weight and chain structure in different. According to this, it can be said that higher coordinated surface titanium and aluminum species are considered to be higher molecular weight Flory component of active sites, which produces higher molecular weight polymer chain due to less chain transfer and chain termination reactions. It can also be said from the MWD curves that higher MW peaks among the multiple peaks

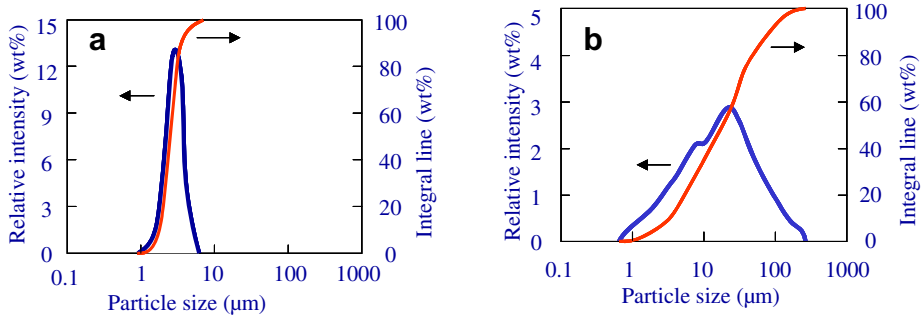

Run No.	Sample	Average particle Size (μm)
1	WG	3.0
2	DG	35.4

Fig. 4. Particle size distribution of AA-$TiCl_3$ based catalysts. (a) WG catalyst (b) DG catalyst.

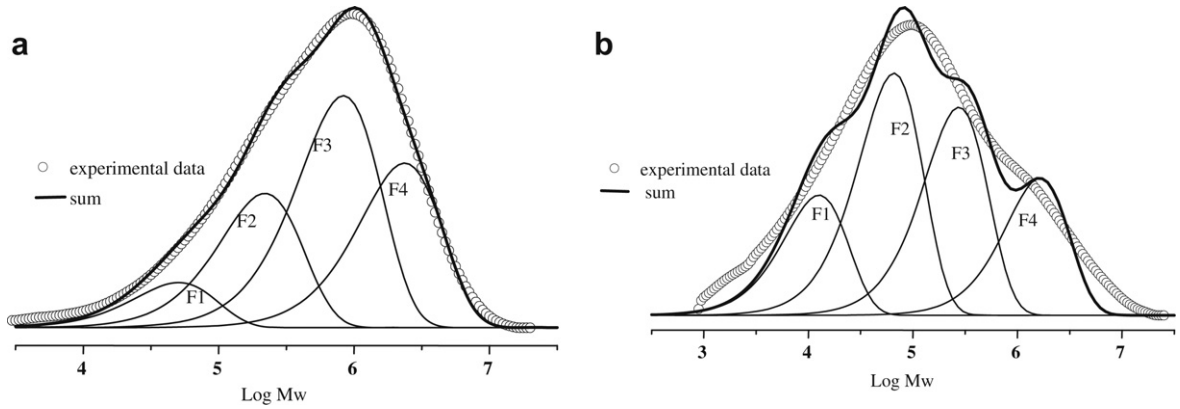

Fig. 6. GPC curves and Flory components of polypropylene prepared with (a) WG AA-$TiCl_3$/DEAC and (b) WG AA-$TiCl_3$/TEA catalyst systems at 40 °C.

of Flory components are assigned to the higher coordination surface Ti- and/or Al-species with higher isospecificity of active sites. The average molecular weights of Flory components differ quite significantly from site to site. As a result, different active sites produce polymer molecules with molecular weight values in the broad ranges. The broad MWD of polypropylene prepared with $MgCl_2$/$TiCl_4$/TEA catalysts can be represented by several Flory components [118]. The procedure for the resolution of complex GPC curves into those of the Flory components were required to describe adequately the MWD. Meanwhile, all the peaks were shifted from lower MW to higher MW after replacing TEA with DEAC. It is due to having higher number of highly coordinated of Ti^{+3}(b) species in the WG $TiCl_3$/DEAC catalyst system.

Therefore, the replacement of TEA as a cocatalyst with DEAC usually results in an increase in the polymer molecular weight. This means that the molecular weights of all Flory components are increased in the polymer with DEAC. From the comparison between two curves, it can be said that the reason for the broad molecular weight distribution of polypropylene produced with TEA is mainly existence of various active sites mainly higher number of Ti^{+3}(a) species, which indicate preferential rate of propagation, chain termination and chain transfer rate constants. The key concept to interpret these phenomena in relation to the cocatalyst concentrations are assuming the existence of at least two kinds of titanium species. The influence of deactivation of the active sites due to the over reduction is the higher the reducing power of the cocatalyst, the greater the deactivation [104]. Thus it can be assumed that a part of the titanium species might be activated easily by the reduction of TEA to generate active sites having easy deactive feature. On the other hand, the catalyst system with DEAC produces narrow ranges molecular weight distribution of polypropylene due to the formation of active sites having lower reduction power and chain termination and transfer ability during polymerization. It has been known for a long time that the replacement of TEA as a cocatalyst with DEAC usually depresses not only the activity but also results in an increase in the polymer molecular weight [119–121].

4. Surface structure vs. microstructure

According to the surface characterization of the catalyst, it was observed that TEA shows lower isospecificity because of the formation of a lower percentage of high-coordinated surface Ti^{3+}(b) species but DEAC represents higher isospecificity due to the formation of a higher percentage of high-coordinated Ti^{3+}(b) species. Moreover, TEA as a cocatalyst shows mostly low coordinated aluminum species (Al^{IV}, Al^{V}) whereas DEAC produces dominantly high-coordinated (Al^{VI}) species. Therefore, the active sites with higher coordinated surface Ti^{3+}(b) species and six-coordinated aluminum species (Al^{VI}), which originated from the interaction with DEAC and wet grinding method of catalyst preparation, show higher isospecificity, which produces a higher fraction of isotactic PP. It is also considered that the highly active Al-alkyl cocatalyst causes a drastic change in the coordination state of the titanium species, resulting in a decrease of the higher coordinated titanium species into lower coordination one. It can be seen from the XPS data analyses that the value of the surface Ti atomic percentage with a higher coordination state is much higher in the case of using DEAC than when using TEA. Depending on the roles of the Al-alkyl cocatalyst and the catalyst preparation method in determining the nature of the isospecificity of active sites, a basic understanding concerning the formation and transformation of isospecific active sites has been achieved.

5. Conclusions

In this study, a detailed experimental approach to the real nature of isospecific sites on a first generation donor- and support-free $TiCl_3$-based Ziegler–Natta catalyst was performed in terms of various catalyst preparation, polymerization, type of Al-alkyl cocatalysts, followed by the systematic characterization of both catalysts and PPs produced. The surface structure of the catalyst analyzed by XPS revealed that two types of Ti^{3+}-species exist on the surface, depending upon the different level of coordination states. The Ti^{3+}(b) species with higher coordination numbers are thought to be the precursors of higher isospecific active sites, which are dominant on the DEAC activated WG AA-$TiCl_3$ catalyst systems; in comparison, the lower coordinated Ti^{3+}(a) species are thought to be the precursors of less isospecific active sites, which are dominant on the TEA activated DG AA-$TiCl_3$ catalyst systems. The coordination state of surface Al compounds complexed with the surface Ti-species was clearly observed as six- (Al^{VI},) five- (Al^{V}) and four- (Al^{IV}) coordination Al, depending on the types of cocatalysts. The polymerization activity, isospecificity and the isospecificity distribution of the active sites of $TiCl_3$ catalysts are dominantly affected by the types of Al-alkyl cocatalysts. In general, higher isospecificity of active sites was demonstrated to be related to higher coordinative states of surface Ti- and Al-species in terms of the type of cocatalyst and preparation method. However, the isospecific nature of surface Ti-species combined with the coordination state of surface Al compounds completely replicates the polymer microisotacticity.

Acknowledgements

The authors are grateful to Toho Catalyst Co. Ltd., Asahi Chemical industry Co. Ltd., Japan Polypropylene Co. Ltd., and Tosoh Finechem. Corp., for their support and donation to our laboratory.

References

[1] Barbé PC, Cecchin G, Noristi L. Adv Polym Sci 1987;81:1.
[2] Moore Jr EP. "The rebirth of polypropylene: supported catalysts". Munich: Hanser Publishers; 1998.
[3] Daniele F, Antonella G, Stefano M, Gian AR, Eugenio T, Silvano B. J Mol Catal A Chem 2002;178:115.
[4] Monaco G, Toto M, Guerra G, Corradini P, Cavallo L. Macromolecules 2000;33:8953.
[5] Sacchi MC, Forlini F, Tritto I, Locatelli P. Macromol Chem Phys 1995;196:2881.
[6] Sacchi MC, Forlini F, Tritto I, Locatelli P, Morini G, Noristi L, et al. Macromolecules 1996;29:3341.
[7] Morini G, Albizzati E, Balbontin G, Mingozzi I, Sacchi MC, Forlini F, et al. Macromolecules 1996;29:5770.
[8] Barino L, Scordamaglia R. Macromol Theory Simul 1998;7:407.
[9] Kojoh S, Kioka M, Kashiwa N. Eur Polym J 1999;35:751.
[10] Boero M, Parrinello M, Terakura K. J Am Chem Soc 2000;122:501.
[11] Kim SH, Somorjai GA. J Phys Chem B 2001;105:3922.
[12] Kim SH, Somorjai GA. J Phys Chem B 2002;106:1386.
[13] Chadwick JC, Morini G, Balbontin G, Camurati I, Heere JJR, Mingozzi I, et al. Macromol Chem Phys; 2001:202. 1995.
[14] Chadwick JC. Macromol Symp 2001;173:21.
[15] Bukatov GD, Zakharov VA. Macromol Chem Phys 2001;202:2003.
[16] Cossee P. J Catal 1964;3:80.
[17] Cossee P. J Catal 1964;3:65.
[18] Ivin KJ, Rooney JJ, Stewart CD, Green MLH, Mahtab R. J Chem Soc Chem Commun; 1978:604.
[19] Brookhart M, Green MLH. J Organomet Chem 1983;250:395.
[20] Mori H, Iguchi H, Hasebe K, Terano M. Macromol Chem Phys 1997;198:1249.
[21] Keii T. Kinetics of Ziegler–Natta polymerization. Tokyo: Kodansha; 1972;
Mori H, Terano M. Trends Polym Sci 1997;5:314;
Maximov NG, Kushnareva EG, Zakharov VA, Anuvrienko VF, Zhdan PA, Yermakov YI. Kinet Katal 1974;15:738.
[22] Mori H, Saito H, Terano M. Macromol Chem Phys 1998;199:55.
[23] Mori H, Saito H, Yamahiro M, Kono H, Terano M. Macromol Chem Phys 1998;199:613.
[24] Yamahiro M, Mori H, Nitta K, Terano M. Macromol Chem Phys 1999;200:134.
[25] Mori H, Yamahiro M, Terano M, Takahashi M, Matsuoka T. Angew Makromol Chem 1999;273:40.
[26] Yamahiro M, Mori H, Nitta K, Terano M. Polymer 1999;40:5265.
[27] Mori H, Yamahiro M, Terano M, Takahashi M, Matsuoka T. Macromol Chem Phys 2000;201:289.
[28] Mori H, Kono H, Terano M. Macromol Chem Phys 2000;201:543.
[29] Kono H, Mori H, Terano M, Nakatani H, Nishiyama I. J Appl Polym Sci 2002;83:2976.
[30] Liu B, Matsuoka H, Terano M. Macromol Rapid Commun 2001;22:1.
[31] Matsuoka H, Liu B, Nakatani H, Terano M. Macromol Rapid Commun 2001;22:326.
[32] Liu B, Matsuoka H, Terano M. Macromol Symp 2001;165:3.
[33] Nitta T, Liu B, Nakatani H, Terano M. J Mol Catal A: Chem 2002;180:25.
[34] Liu B, Nitta T, Nakatani H, Terano M. Macromol Chem Phys 2002;203:2412.
[35] Corradini P, Villani V, Guerra G. Macromolecules 1985;18:1041.
[36] Busico V, Corradini P, Martino L, Proto A, Savino V. Macromol Chem 1985;186:1279.
[37] Busico V, Corradini P, Ferrara A, Proto A. Macromol Chem 1986;187:1115.
[38] Busico V. Macromol Chem 1986;187:1125.
[39] Busico V. Macromol Chem 1991;191:49.
[40] Corradini P, Busico V, Cipullo R. Stud Surf Sci Catal 1994;89:21.
[41] Mori H, Terano M. In: Sano T, Uozumi T, Nakatani H, Terano M, editors. Progress and development of catalytic olefin polymerization. Tokyo: Technology and Education Publishers; 2000. p. 65.
[42] Soares JBP, Hamielec AE. Polymer 1996;37:4607.
[43] Keii T. Macromol Theory Simul 1995;4:947.
[44] Magni E, Somorjai GA. Catal Lett 1995;35:205.
[45] Magni E, Somorjai GA. Surf Sci 1995;341:L1078.
[46] Magni E, Somorjai GA. J Phys Chem 1996;100:14786.
[47] Magni E, Somorjai GA. Surf Sci 1997;377:824.
[48] Magni E, Somorjai GA. J Phys Chem B 1998;102:8788.
[49] Korànye TI, Magni E, Somorjai GA. Top Catal 1999;7:179.
[50] Hasebe K, Mori H, Terano M. J Mol Catal A Chem 1997;124:L1.
[51] Mori H, Hasebe K, Terano M. Polymer 1999;40:1389.
[52] Mori H, Hasebe K, Terano M. J Mol Catal A Chem 1999;140:165.
[53] Thune PC, Loos J, Lemstra PJ, Niemantsverdriet JW. J Catal 1999;83:1.
[54] Ville V, Pasi L, Päivi P, Franciska S. Polymer 2004;45:3091.
[55] Giunchi G, Clementi E, Ruiz-Vizcaya ME, Novaro O. Chem Phys Lett 1977;49:8.
[56] Novaro O, Blaisten-Barojas E, Clementi E, Giunchi G, Ruiz-Vizcaya ME. J Chem Phys 1978;58:2337.
[57] Fujimoto H, Yamasaki T, Mizutani H, Koga N. J Am Chem Soc 1985;107:6157.
[58] Sakai S. J Phys Chem 1994;98:12053.
[59] Jensen VR, Borve KJ, Ystenes M. J Am Chem Soc 1995;117:9.
[60] Lin JS, Catlow CRA. J Catal 1995;157:145.
[61] Cavallo L, Guerra G, Corradini P. J Am Chem Soc 1998;120:2428.
[62] Gale JD, Catlow CRA, Gillan MJ. Top Catal 1999;9:235.
[63] Puhakka E, Pakkanen TT, Pakkanen TA. Surf Sci 1995;334:289.
[64] Puhakka E, Pakkanen TT, Pakkanen TA. J Mol Catal A 1997;120:143.
[65] Shiga A, Kawamura-Kuribayashi H, Sasaki T. J Mol Catal A 1995;98:15.
[66] Boero M, Parrinello M, Terakura K. J Am Chem Soc 1998;120:2746.
[67] Boero M, Parrinello M, Hüffer S, Weiss H. J Am Chem Soc 2000;1222:501.
[68] Boero M, Parrinello M, Hüffer S, Weiss H. J Phys Chem A 2001;105:5096.
[69] Weiss H, Boero M, Parrinello M. Macromol Symp 2001;173:137.
[70] Toto M, Morini G, Guerra G, Corradini P, Cavallo L. Macromolecules 2000;33:1134.
[71] Viville P, Daous D, Jonas AM, Nysten B, Legras R, Dupire M, et al. Polymer 2001;42:1953.
[72] Corradini P, Barone V, Fusco R, Guerra G. Gazz Chim Ital 1983;113:601.
[73] Corradini P, Guerra G. Prog Polym Sci 1991;16:239.
[74] Busico V, Corradini P, Martini LD, Proto A, Albizzati E. Makromol Chem 1986;187:1115.
[75] Busico V, Corradini P, Martino LD, Proto A, Savino V, Albizzati E. Makromol Chem 1985;186:1279.
[76] Busico V, Chipullo R, Corradini P, Biasio RD. Macromol Chem Phys 1995;196:491.
[77] Soga K, Shiono T, Doi Y. Makromol Chem 1988;189:1531.
[78] Kakugo M, Miyatake T, Naito Y, Mizunuma K. In: Quirk RP, editor. Transition metal catalyzed polymerization, Ziegler–Natta and metathesis polymerizations. Cambridge: Cambridge University Press; 1988. p. 624.
[79] Miyatake T, Mizunuma K, Kakugo M. In: Keii T, Soga K, editors. Catalytic olefin polymerization, 56. Amsterdam: Elsevier; 1990. p. 155.
[80] Soares JBP. Chem Eng Sci 2001;56:4131.
[81] Furuta M. J Polym Sci Polym Phys 1981;19:135.
[82] Gassman PC, Callstrom MR. J Am Chem Soc 1987;109:7875.
[83] Hasan ATMK, Liu B, Terano M. Polym Bull 2005;54:225.
[84] Hasan ATMK, Wang Q, Liu B, Terano M. 2008; Sankeisha ISBN978-4-88361-616-9 C3058 p. 44–51.
[85] Kim SH, Somorjai GA. Surf Interface Anal 2001;31:701.
[86] Desbuquoit CM, Riga J, Verbist JJ. J Chem Phys 1983;79:26.
[87] Desbuquoit CM, Riga J, Verbist JJ. Inorg Chem 1987;26:1212.
[88] Somorjai GA, Kim SH. Appl Surf Sci 2000;161:333;
Somorjai GA, Kim SH. J Phys Chem B 2000;104:5519.
[89] Arlman EJ. J Cat 1966;5:178.
[90] Mori H, Yoshitome M, Terano M. Macromol Chem Phys 1997;198:3207;
Mori H, Yoshitome M, Terano M. Macromol Chem Phys 2000;201:298.
[91] Rodriguez LAM, Van Looy HM, Gabant JA. J Polym Sci A-1 1966;4:1905.
[92] Cossee P. Tetrahedron 1960;17:12.
[93] Okura I, Sendoda Y, Keii T. Tetrahedron 1970;73:276.
[94] Boor Jr J. Macromol Rev 1967;2:115.
[95] Arlman EJ. J Catal 1964;3:89.
[96] Wilchinsky ZW, Looney RW, Tornqvist EGM. J Catal 1973;28:351.
[97] Tornqvist EGM. Ann NY Acad Sci 1969;155:447.
[98] Tornqvist EGM, Richardson JT, Wilchinsky ZW, Looney RW. J Catal 1967;8:189.
[99] Fregonese D, Glisenti A, Mortara S, Rizzi GA, Tondello E, Bresadola S. J Mol Catal A Chem 2002;178:115.
[100] (a) Mori H, Kono H, Terano M, Nosov A, Zakharov VA. J Mol Catal A Chem 2000;164:235;
(b) Liu B, Fukuda K, Nakatani H, Nishiyama I, Yamahiro M, Terano M. J Mol Catal A: Chem 2004;219:363.
[101] Veselý K, Ambrož J, Mejzlík J, Spousta E. J Polym Sci Part C 1967;16:417.
[102] Seppälä JV, Auer M. Prog Polym Sci 1990;15:147;
Soga K, Yanagihara HY, Lee DH. Makromol Chem 1989;190:995.
[103] (a) Potapov AG, Kriventsov VV, Bukatov GD, Zakharov VA. J Mol Catal A Chem 1997;122:61;
(b) Potapov AG, Kriventsov VV, Kochubey D, Bukatov GD, Zakharov VA. Macromol Chem Phys 1997;198:3477.
[104] Ohnishi K, Mori H, Terano M. Macromol Chem Phys 1998;199:393.
[105] Benn R, Zanssen E, Lehmkuhl H, Rafinska A. J Organomet Chem 1987;333:155.
[106] Černý Z, Macháček J, Fusek J, Heřmánek S, Kříž O, Čásenký B. J Organomet Chem 1991;402:141.
[107] Mackie P, Berger MN, Grieveson BM, Lawson D. Polym Lett 1967;5:493;
Putanov P, Kiss E, Fekete L, Dingova E. Polyhedron 1989;8:1967;
Bailly JC, Hagege R. Polymer 1991;32:181.
[108] Cossee P. Tetrahedron Lett 1960;17:12.
[109] Chien JCW, Wu J, Kuo C. J Polym Sci Polym Chem Ed 1983;21:737;
Chien JCW. Catal Rev Sci Eng 1984;26:613.
[110] Firsov AP, Sandomirskaya ND, Tsvetkova VI, Chirkov NM. Vysokomol Soedin 1961;3:1352.
[111] Vesely K, Ambroz J, Hamric O. J Polym Sci Part C 1963;4:11.
[112] Chumaevsky NB, Zakharov VA, Bukativ GB, Kuznetsova GI, Yermakov YI. Makromol Chem 1976;177:747.
[113] Kollar L, Simon A, Kallo A. J Polym Sci Part A-1 1968;6:937.
[114] Kakugo M, Miyatake T, Naito Y, Mizunuma K. Macromolecules 1988;21:314.
[115] Keii T. Stud Surf Sci Catal 1990;56:1.
[116] Kissin YV. Makromol Chem Macromol Symp 1993;66:83;
Kissin YV. J Polym Sci Part A Polym Chem 1995;33:227. Kissin YV. J Polym Sci Part A Polym Chem 2003;41:1745;
Kissin YV, Francis MM, Craig CM. J Polym Sci Part A: Polym Chem 2005;43:4351.
[117] Fan ZQ, Feng LX, Yang SL. J Polym Sci Part 4 Polym Chem 1996;34:3329;
Fan ZQ, Yang K, Deng HY, Jiang X. Polymer 2003;42:5559.
[118] Kissin YV. J Polym Sci Part A: Polym Chem 2001;39:1681.
[119] Busico V, Chipullo R, Monaco G, Vacatello M. Macromolecules 1997;30:6251.
[120] McKnight AL, Masood MA, Waymouth RM, Strauss DA. Organometallics 1997;16:2879.
[121] McKnight AL, Waymouth RM. Chem Rev 1998;98:2587.